Electrocommunication for weakly electric fish

A. Scapin

ELECTROCOMMUNICATION FOR WEAKLY ELECTRIC FISH

ANDREA SCAPIN

ABSTRACT. This paper addresses the problem of the electro-communication for weakly electric fish. In particular we aim at sheding light on how the fish circumvent the jamming issue for both electro-communication and active electro-sensing. A real-time tracking algorithm is presented.

1. INTRODUCTION

In this paper we address the problem of studying the behaviour of two weakly electric fish when they populate the same environment. Those kind of animals orient themselves at night in complete darkness by using their active electro-sensing system. They generate a stable, relatively high-frequency, weak electric field and transdermically perceive the corresponding feedback by means of many receptors on its skin. Since they have an electric sense that allows underwater navigation, target classification and intraspecific communication, they are privileged animals for bio-inspiring man-built autonomous systems [14, 18, 19, 21, 24, 29, 39, 40]. For electro-communication purposes, in processing sensory information, this system has to separate feedback associated with their own signals from interfering sensations caused by signals from other animals. Wave and pulse species employ different mechanisms to minimize interference with EODs of conspecifics. It has been observed that certain wave species, having wave-type electric organ discharge (EOD) waveforms, such as Eigenmannia and Gymnarchus, reflexively shift their EOD frequency away from interfering frequencies of nearby conspecifics, in order to avoid "jamming" each others electrical signals. This phenomenon is known as *jamming avoidance response* (JAR) [13, 22, 23]. The electro-communication for the weakly electric fish has already been studied in the case of a simplified model consisting of a dipole-dipole interaction [39].

A lot of effort has also been devoted to the electro-sensing problem, that is, the capability of the animal to detect and recognize a dielectric target nearby [26, 31, 8, 9, 12, 16, 27, 28, 32, 35, 36, 37]. For the mathematical model of the electric fish described in [2], it has been shown that the fish is able to locate a small target by employing a MUSIC-type algorithm based on a multi-frequency approach. Its robustness with respect to measurement noise and its sensitivity with respect to the number of frequencies, the number of sensors, and the distance to the target have also been illustrated. The classification capabilities of the electric fish have also been investigated. In particular, invariant quantities under rotation, translation and scaling of the target, based on the generalized polarization tensors (GPTs), have been derived and used to identify a small homogeneous target among other shapes of a pre-fixed dictionary [3, 4, 5, 6, 7]. The stability of the identifying procedure has been discussed. The recognition algorithm has been recently extended to sense small inhomogeneous target [33]. In [10], a capacitive sensing method has recently

---

been implemented. It has been shown that the size of a capacitive sphere can be estimated from multi-frequency electrosensory data. In [11], uniqueness and stability estimates to the considered electro-sensing inverse problem have been established.

In the present work we designed and implemented a real-time tracking algorithm for a fish to track another conspecific that is swimming nearby. In particular, we showed that the following fish can sense the presence of the leading fish and can estimate its positions by using a MUSIC-type algorithm for searching its electric organ. We also showed that the fish can locate a small dielectric target which lies in its electro-sensing range even when another fish is swimming nearby, by filtering out its interfering signal and by applying the MUSIC-type algorithm developed in [2].

The paper is organized as follows. In Section 2, starting from Maxwell's equations in time domain we adapt the mathematical model of the electric fish proposed in [2] in order to be able to consider many fish with EOD working at possibly different frequencies. We give a decomposition formula for the potential and, as a consequence, we decouple the dipolar signals of the two fish when they have different EOD fundamental frequencies. The amplitude of each signal can be retrieved from the measurements using Fourier analysis techniques.

In Section 3, we use the decomposition formula for the total signal to tackle the problem in the frequency domain. This allows us to employ a non-iterative MUSIC-type dipole search algorithm for a fish to track another fish of the same species nearby.

In Section 4, we provide a method for a fish to electro-sense a small dielectric target in the presence of many conspecifics. The aim of this section is to locate the target which making use of the dipolar approximation of the transdermal potential modulations. We show that the multi-frequency MUSIC-type algorithm in [5] is still applicable after decomposing the total signal.

In Section 5, many numerical simulations are driven. The performances of the real-time tracking algorithm are reported. We show that the algorithms work well even when the measurements are corrupted by noise.

2. The two-fish model and the jamming avoidance response

Let Ω be a simply-connected bounded domain. We assume $\Omega \in C^{2,\alpha}$ for some $0 < \alpha < 1$. Given an arbitrary function w defined on $\mathbb{R}^2 \setminus \partial\Omega$ and $x \in \partial\Omega$, we define

$$w(x)|_{\pm} := \lim_{t \to 0} w(x \pm t\nu(x)),$$

$$\frac{\partial w}{\partial \nu}(x)\bigg|_{\pm} := \lim_{t \to 0} \nabla w(x \pm t\nu(x)) \cdot \nu(x),$$

where ν is the outward normal to $\partial\Omega$.
Let us denote by Γ the fundamental solution of the Laplacian in $\mathbb{R}^2$, that is,

$$\Gamma(x - y) = \frac{1}{2\pi} \log \|x - y\|, \quad x \neq y \in \mathbb{R}^2.$$

The single- and double-layer potentials on Ω, $\mathcal{S}_\Omega$ and $\mathcal{D}_\Omega$, are the operators that respectively map any $\phi \in L^2(\partial\Omega)$ to

$$\mathcal{S}_\Omega[\phi](x) = \int_{\partial\Omega} \Gamma(x, y)\phi(y) \, \mathrm{d}s_y,$$

$$\mathcal{D}_\Omega[\phi](x) = \int_{\partial\Omega} \frac{\partial \Gamma}{\partial \nu_y}(x, y)\phi(y) \, \mathrm{d}s_y.$$

Recall that for $\phi \in L^2(\partial\Omega)$, the functions $\mathcal{S}_{\partial\Omega}[\phi]$ and $\mathcal{D}_{\partial\Omega}[\phi]$ are harmonic functions in $\mathbb{R}^2 \setminus \partial\Omega$.

The behaviour of these functions across the boundary $\partial\Omega$ is described by the following relations [1]:

$$\mathcal{S}_\Omega[\phi]|_+ = \mathcal{S}_\Omega[\phi]|_-,$$

$$\left.\frac{\partial \mathcal{S}_\Omega[\phi]}{\partial \nu}\right|_\pm = \left(\pm\frac{1}{2}I + \mathcal{K}_\Omega^*\right)[\phi],$$

$$\mathcal{D}_\Omega[\phi]|_\pm = \left(\mp\frac{1}{2}I + \mathcal{K}_\Omega\right)[\phi],$$

$$\left.\frac{\partial \mathcal{D}_\Omega[\phi]}{\partial \nu}\right|_+ = \left.\frac{\partial \mathcal{D}_\Omega[\phi]}{\partial \nu}\right|_-.$$

The operator $\mathcal{K}_\Omega$ and its L^2-adjoint $\mathcal{K}_\Omega^*$ are given by the following formulas:

$$(2.1) \qquad \mathcal{K}_\Omega[\phi](x) := \frac{1}{2\pi} \int_{\partial\Omega} \frac{(y-x)\cdot\nu(y)}{|x-y|^2}\phi(y)\,\mathrm{d}s_y, \qquad x \in \partial\Omega,$$

$$(2.2) \qquad \mathcal{K}_\Omega^*[\phi](x) := \frac{1}{2\pi} \int_{\partial\Omega} \frac{(x-y)\cdot\nu(x)}{|x-y|^2}\phi(y)\,\mathrm{d}s_y, \qquad x \in \partial\Omega.$$

For the sake of simplicity, we consider the case of two weakly electric fish $\mathfrak{F}_1$ and $\mathfrak{F}_2$. The extension to the case of many fish is immediate.

Starting from Maxwell's equations in time domain we derive

$$\nabla \cdot (\sigma + \varepsilon\partial_t)E = -\nabla \cdot j_s \quad \text{in } \mathbb{R}^2,$$

where σ is the conductivity of the medium, ε is the electric permittivity, E is the electric field, j_s is a source of current. Let ω_1 and ω_2 be the fundamental frequencies associated to the oscillations of the electric organ discharge (EOD) of the two fish $\mathfrak{F}_1$ and $\mathfrak{F}_2$, respectively. We consider a source term which is of the form

$$-\nabla \cdot j_s = e^{i\omega_1 t}f_1(x) + e^{i\omega_2 t}f_2(x),$$

where $f_1 = \sum \alpha_j^{(1)}\delta_{x_j^{(1)}}$ and $f_2 = \sum \alpha_j^{(2)}\delta_{x_j^{(2)}}$ are the spatial dipoles located inside Ω_1 and Ω_2, respectively. Throughout this paper we assume that the dipoles f_1 and f_2 satisfy the local charge neutrality conditions:

$$\alpha_1^{(i)} + \alpha_2^{(i)} = 0 \quad \text{for } i = 1\,;$$

see [2]. Considering the boundary conditions as in [2], we get the following system of equations:

$$(2.3) \quad \begin{cases} \Delta u(x,t) = f_1(x)h_1(t) & \text{in } \Omega_1 \times \mathbb{R}^+, \\ \Delta u(x,t) = f_2(x)h_2(t) & \text{in } \Omega_2 \times \mathbb{R}^+, \\ \nabla \cdot (\sigma(x) + \varepsilon(x)\partial_t)\nabla u(x,t) = 0 & \text{in } (\mathbb{R}^2 \setminus \overline{\Omega_1 \cup \Omega_2}) \times \mathbb{R}^+, \\ u|_+ - u|_- = \xi_1 \left.\dfrac{\partial u}{\partial \nu}\right|_+ & \text{on } \partial\Omega_1 \times \mathbb{R}^+, \\ u|_+ - u|_- = \xi_2 \left.\dfrac{\partial u}{\partial \nu}\right|_+ & \text{on } \partial\Omega_2 \times \mathbb{R}^+, \\ \left.\dfrac{\partial u}{\partial \nu}\right|_- = 0 & \text{on } \partial\Omega_1 \times \mathbb{R}^+, \partial\Omega_2 \times \mathbb{R}^+, \\ |u(x,t)| = O(|x|^{-1}) & \text{as } |x| \to \infty,\ t \in \mathbb{R}^+, \end{cases}$$

where σ_0, ε_0 are the material parameters of the target D, and ξ_1 and ξ_2 are the effective skin thickness parameters of $\mathfrak{F}_1$ and $\mathfrak{F}_2$, respectively. Here, h_1 and h_2 encode the type of signal generated by the fish.

2.1. **Wave-type fish.** For the wave-type fish we have $h_1(t) = e^{i\omega_1 t}$ and $h_2(t) = e^{i\omega_2 t}$. When $\omega_1 \neq \omega_2$ the overall signal is the superposition of two periodic signals oscillating at different frequencies.

Proposition 2.1. *If $\omega_1 \neq \omega_2$ such that $\omega_1, \omega_2 \neq 0$, then the solution u to the equations* (2.3) *can be represented as*

$$(2.4) \qquad u(x,t) = u_1(x)e^{i\omega_1 t} + u_2(x)e^{i\omega_2 t},$$

where u_1, u_2 satisfy the following transmission problems:

$$(2.5) \quad \begin{cases} \Delta u_1(x) = f_1(x) & \text{in } \Omega_1, \\ \Delta u_1(x) = 0 & \text{in } \Omega_2, \\ \nabla \cdot (\sigma(x) + i\omega_1 \varepsilon(x))\nabla u_1(x) = 0 & \text{in } \mathbb{R}^2 \setminus \overline{\Omega_1 \cup \Omega_2}, \\ u_1|_+ - u_1|_- = \xi_1 \dfrac{\partial u_1}{\partial \nu}\Big|_+ & \text{on } \partial\Omega_1, \\ u_1|_+ - u_1|_- = \xi_2 \dfrac{\partial u_1}{\partial \nu}\Big|_+ & \text{on } \partial\Omega_2, \\ \dfrac{\partial u_1}{\partial \nu}\Big|_- = 0 & \text{on } \partial\Omega_1, \partial\Omega_2, \\ |u_1(x)| = O(|x|^{-1}) & \text{as } |x| \to \infty, \end{cases}$$

and

$$(2.6) \quad \begin{cases} \Delta u_2(x) = 0 & \text{in } \Omega_1, \\ \Delta u_2(x) = f_2(x) & \text{in } \Omega_2, \\ \nabla \cdot (\sigma(x) + i\omega_2 \varepsilon(x))\nabla u_2(x) = 0 & \text{in } \mathbb{R}^2 \setminus \overline{\Omega_1 \cup \Omega_2}, \\ u_2|_+ - u_2|_- = \xi_1 \dfrac{\partial u_2}{\partial \nu}\Big|_+ & \text{on } \partial\Omega_1, \\ u_2|_+ - u_2|_- = \xi_2 \dfrac{\partial u_2}{\partial \nu}\Big|_+ & \text{on } \partial\Omega_2, \\ \dfrac{\partial u_2}{\partial \nu}\Big|_- = 0 & \text{on } \partial\Omega_1, \partial\Omega_2, \\ |u_2(x)| = O(|x|^{-1}) & \text{as } |x| \to \infty. \end{cases}$$

Proof. We substitute (2.4) into (2.3). Considering the equation in $\Omega_1 \times \mathbb{R}^+$ we get

$$e^{i\omega_1 t}\Delta u_1 + e^{i\omega_2 t}\Delta u_2 = e^{i\omega_1 t} f_1.$$

Thus

$$(\Delta u_1 - f_1) + e^{i(\omega_2 - \omega_1)t}\Delta u_2 = 0,$$

which yields $\Delta u_1 - f_1 = 0$ in Ω_1 and $\Delta u_2 = 0$ in Ω_1.
In the same manner, we get the equations satisfied by u_1 and u_2 in Ω_2.
Outside the fish bodies, we have

$$\nabla \cdot (\sigma + \varepsilon\partial_t)\nabla e^{i\omega_1 t} u_1 + \nabla \cdot (\sigma + \varepsilon\partial_t)\nabla e^{i\omega_2 t} u_2 = 0,$$

$$e^{i\omega_1 t}\nabla \cdot (\sigma + i\omega_1\varepsilon)\nabla u_1 + e^{i\omega_2 t}\nabla \cdot (\sigma + i\omega_2\varepsilon)\nabla u_2 = 0,$$

that yields $\nabla \cdot (\sigma + i\omega_1\varepsilon)\nabla u_1 = 0$ in $\mathbb{R}^2 \setminus (\overline{\Omega_1 \cup \Omega_2})$ and $\nabla \cdot (\sigma + i\omega_2\varepsilon)\nabla u_2 = 0$ in $\mathbb{R}^2 \setminus (\overline{\Omega_1 \cup \Omega_2})$.

Finally it is easy to check that the boundary conditions remain unchanged because the time dependency does not appear explicitly.

$\square$

Remark. The potentials u_1 and u_2, that respectively solve (2.5) and (2.6), have a meaningful interpretation that is based on two different sub-modalities of the electroreception. As a matter of fact, u_1 can be viewed as the potential when the fish $\mathfrak{F}_1$ is active and $\mathfrak{F}_2$ is passive, whereas u_2 can be viewed as the potential when the fish $\mathfrak{F}_1$ is passive and $\mathfrak{F}_2$ is active. See [15].

Formula (2.4) tells us that it is possible to study the total field looking separately at these two different oscillating regimes.

The idea is to separate the two signals from the measurements of their superposition. This can be done easily by using signal analysis techniques, see [17].

Figure 2.3 illustrates the potential before the jamming avoidance response, when the fish emit signals at a certain common frequency, whereas Figure 2.4 depicts the two submodalities contained in the total signal $u(x,t)$ after they have switched their EOD frequencies.

2.2. **Pulse-type fish.** For the pulse-type fish we have that $h_1(t)$ and $h_2(t)$ are pulse wave. We can assume that they both can be obtained from a standard pulse shape $h(t)$ (see Figure Figure 2.1) by means of translation and scaling, i.e.,

$$h_1(t) = h(\eta_1 t - T_1),$$
$$h_2(t) = h(\eta_2 t - T_2).$$
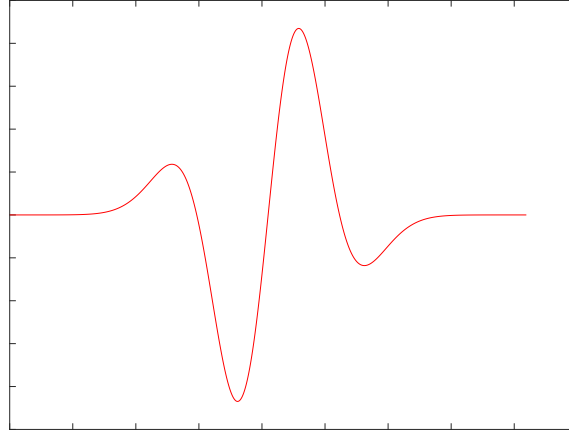
Figure 2.1. Standard shape of the pulse wave $h(t)$.

For some pulse-type species, as Gymnotoid, the jamming avoidance response is obtained by shortening the duration of the emitted pulse, see [23]. In this way, they minimize the chance of pulse coincidence by transient accelerations (decelerations) of their EOD rate. For $\eta_1, \eta_2 > 0$ large enough such that $\text{supp}(h_1) \cap \text{supp}(h_2) = \emptyset$.

Thus, for $t_1, t_2 > 0$ such that $h_1(t_1) \neq 0$ and $h_2(t_2) \neq 0$ we can consider $u_1(x) := u(x, t_1)$ and $u_2(x) := u(x, t_2)$. These time-slices have the following property:

$$\begin{cases} \Delta u_1(x) = f_1(x)h_1(t_1), & x \in \Omega_1 \\ \Delta u_1(x) = 0, & x \in \Omega_2, \end{cases} \quad \begin{cases} \Delta u_2(x) = 0, & x \in \Omega_1 \\ \Delta u_2(x) = f_2(x)h_2(t_2), & x \in \Omega_2 \end{cases}.$$

Hence we can achieve a separation of signals.
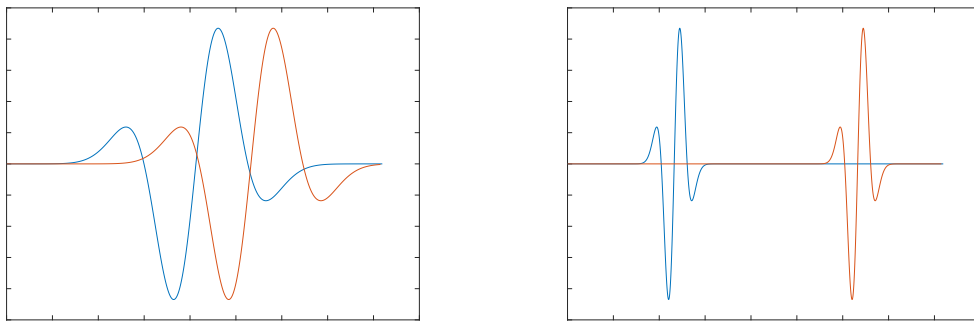
**(a)** Before the JAR the two pulse signals may interfere with each other.

(b) By shortening the duration of the pulse it is possible to identify two non-overlapping time-windows I_1 and I_2 corresponding to the signal emitted by the fish $\mathfrak{F}_1$ and $\mathfrak{F}_2$, respectively.

Figure 2.2

In the next sections, we will see an important consequence of Proposition 2.1. As a matter of fact $\mathfrak{F}_1$ can track $\mathfrak{F}_2$ by using the measurements of $u_2|_{\partial\Omega_1}$, solution to (2.6), and can detect a small target D by using the measurements of $u_1|_{\partial\Omega_1}$.
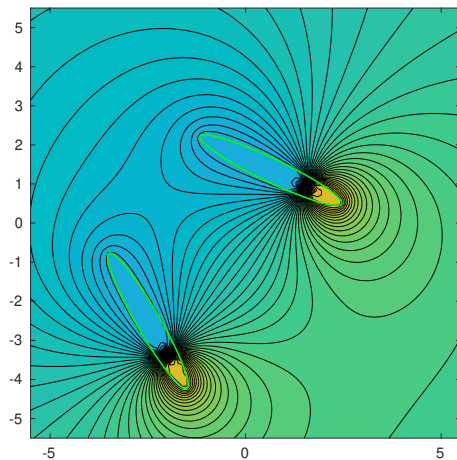
Figure 2.3. Before the JAR (the EOD frequencies of the two fish are the same). Plot of $u(x) = u_1(x) + u_2(x)$, where $u(x,t) = u(x)e^{i\omega_0 t}$.
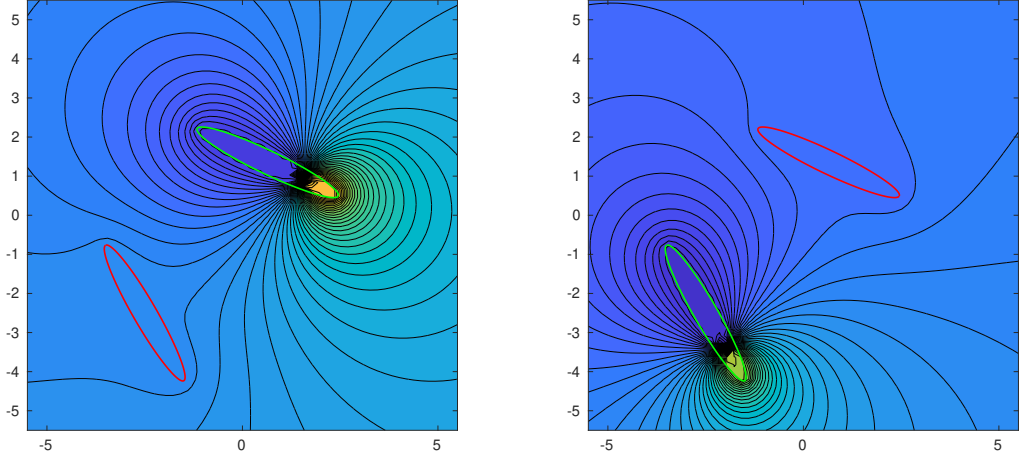
(a) Plot of u_2. Ω_1 (red) is passive and Ω_2 (green) is active.

(b) Plot of u_1. Ω_1 (green) is active and Ω_2 (red) is passive.

Figure 2.4. After the JAR (the EOD frequencies ω_1 and ω_2 of the two fish are apart from each other).

3. Electro–communication

The aim of this section is to give a mathematical procedure to model the communication abilities of the weakly electric fish, i.e., the capability of a fish to perceive a conspecific nearby. Assume, for instance, the point of view of the fish $\mathfrak{F}_1$. We want $\mathfrak{F}_1$ to estimate some basic features of $\mathfrak{F}_2$, such as the position of its electric organ. More importantly, by using subsequent estimates, we want to design an algorithm for $\mathfrak{F}_1$ to track $\mathfrak{F}_2$.

For the sake of clarity, we consider the case without the small dielectric target. It is worth emphasizing that the presence of the target is not troublesome since its effect on the tracking procedure is negligible even when the fish are swimming nearby.

When $\mathfrak{F}_1$ gets close to $\mathfrak{F}_2$, both $\mathfrak{F}_1$ and $\mathfrak{F}_2$ experiment the so-called jamming avoidance response and thus their electric organ discharge (EOD) frequencies switch. When the EOD frequencies ω_1 and ω_2 are apart from each other, Proposition 2.1 can be applied. Let u_2 be the solution to the transmission problem (2.6). As previously mentioned, the function u_2 can be extracted from the total signal $u(x,t)$ using signal analysis techniques.

We define

$$H^{u_2}(x) = (\mathcal{S}_{\Omega_1} - \xi_1 \mathcal{D}_{\Omega_1}) \left[\left. \frac{\partial u_2}{\partial \nu} \right|_+ \right](x).$$

Let us recall the following boundary integral representation: for each $x \in \mathbb{R}^2 \setminus (\overline{\Omega_1 \cup \Omega_2})$,

$$(u_2 - H^{u_2})(x) = \int_{\partial\Omega_2} \left(\left. \frac{\partial u_2}{\partial \nu} \right|_+ (y)\, \Gamma(x,y) - \frac{\partial \Gamma}{\partial \nu_y}(x,y)\, u_2|_+(y) \right) \mathrm{d}s_y\,.$$

Making use of the Robin boundary condition on $\partial\Omega_2$ and integration by parts yields

$$
\begin{aligned}
(u_2 - H^{u_2})(x) &= \int_{\partial\Omega_2} \left(\left.\frac{\partial u_2}{\partial \nu}\right|_+ (y)\, \Gamma(x,y) - \frac{\partial\Gamma}{\partial\nu_y}(x,y)\, u_2|_+(y) \right) \mathrm{d}s_y \\
&= \int_{\partial\Omega_2} \left(\left.\frac{\partial u_2}{\partial \nu}\right|_+ (y)\, \Gamma(x,y) - \frac{\partial\Gamma}{\partial\nu_y}(x,y) \left(\xi_2 \left.\frac{\partial u_2}{\partial \nu}\right|_+ (y) + u_2|_-(y) \right) \right) \mathrm{d}s_y \\
&= \int_{\partial\Omega_2} \left.\frac{\partial u_2}{\partial \nu}\right|_+ (y) \left(\Gamma(x,y) - \xi_2\frac{\partial\Gamma}{\partial\nu_y}(x,y) \right) \mathrm{d}s_y - \int_{\partial\Omega_2} \frac{\partial\Gamma}{\partial\nu_y}(x,y) u_2|_-(y)\, \mathrm{d}s_y \\
&= \int_{\partial\Omega_2} \left.\frac{\partial u_2}{\partial \nu}\right|_+ \left(\Gamma - \xi_2\frac{\partial\Gamma}{\partial\nu} \right) \mathrm{d}s \pm \alpha \left[\Gamma(x - x_1^{(2)}) - \Gamma(x - x_2^{(2)}) \right].
\end{aligned}
$$

Therefore, we obtain

$$
(3.1) \quad (u_2 - H^{u_2})(x) = \int_{\partial\Omega_2} \left.\frac{\partial u_2}{\partial \nu}\right|_+ \left(\Gamma - \xi_2\frac{\partial\Gamma}{\partial\nu} \right) \mathrm{d}s \pm \alpha \left[\Gamma(x - x_1^{(2)}) - \Gamma(x - x_2^{(2)}) \right].
$$

Observe that, for x away from the $x_1^{(i)}$, we can approximate $\Gamma(x - x_2^{(2)}) - \Gamma(x - x_1^{(2)})$ as follows:

$$
\left[\Gamma(x - x_2^{(2)}) - \Gamma(x - x_1^{(2)}) \right] \approx \pm\nabla\Gamma(x - x_1^{(2)}) \cdot (x_2^{(2)} - x_1^{(2)}) = \frac{(x - x_1^{(2)}) \cdot (x_2^{(2)} - x_1^{(2)})}{\|x - x_1^{(2)}\|^2}.
$$

Consider an array of receptors $(x_l)_{l=1}^M$ on $\partial\Omega_1$. We aim at solving the inverse source problem of determining the dipole, of $\mathfrak{F}_2$ from the knowledge of the measurements on the skin of $\mathfrak{F}_1$:

$$
(3.2) \qquad \left\{ (u_2 - H^{u_2})(x_l) \ : \ \text{for } l = 1, ..., N \right\}.
$$

In order to estimate the dipole, we assume that the following single-dipole approximation holds:

$$
(3.3) \qquad (u_2 - H^{u_2})(x_l) \approx \frac{(x_l - \widehat{z}) \cdot \widehat{\mathbf{p}}}{\|x_l - \widehat{z}\|^2},
$$

where $\widehat{\mathbf{p}}$ and $\widehat{z}$ denote respectively the moment and the center of the equivalent dipolar source.

Remark. The single-dipole approximation (3.3) is an equivalent representation of a spread source. However, in the presence of several well-separated sources, such approximation is not trustworthy anymore [20]. In the case of $P \geq 3$ conspecifics we would extract $u_1, ..., u_P$ components from the total signal, and the single-dipole approximation remains applicable to each one of the components $u_2, ..., u_P$.

4. Electro–sensing

Now, suppose to have $\mathfrak{F}_1, \mathfrak{F}_2$ as before and a target close to $\mathfrak{F}_1$.

Let u_1 be the solution to the transmission problem (2.5), that is,

$$
\begin{cases}
\Delta u_1(x) = f_1(x) & \text{in } \Omega_1, \\
\Delta u_1(x) = 0 & \text{in } \Omega_2, \\
\nabla \cdot (\sigma(x) + i\omega_1\varepsilon(x))\nabla u_1(x) = 0 & \text{in } \mathbb{R}^2 \setminus \overline{\Omega_1 \cup \Omega_2}, \\
u_1|_+ - u_1|_- = \xi_1 \dfrac{\partial u_1}{\partial \nu}\Big|_+ & \text{on } \partial\Omega_1, \\
u_1|_+ - u_1|_- = \xi_2 \dfrac{\partial u_1}{\partial \nu}\Big|_+ & \text{on } \partial\Omega_2, \\
\dfrac{\partial u_1}{\partial \nu}\Big|_- = 0 & \text{on } \partial\Omega_1, \partial\Omega_2, \\
|u_1(x)| = O(|x|^{-1}) & \text{as } |x| \to \infty,
\end{cases}
$$

and let U_1 be the background solution, that solves the problem

$$
\begin{cases}
\Delta U_1(x) = f_1(x) & \text{in } \Omega_1, \\
\Delta U_1(x) = 0 & \text{in } \Omega_2, \\
\Delta U_1(x) = 0 & \text{in } \mathbb{R}^2 \setminus \overline{\Omega_1 \cup \Omega_2}, \\
U_1|_+ - U_1|_- = \xi_1 \dfrac{\partial U_1}{\partial \nu}\Big|_+ & \text{on } \partial\Omega_1, \\
U_1|_+ - U_1|_- = \xi_2 \dfrac{\partial U_1}{\partial \nu}\Big|_+ & \text{on } \partial\Omega_2, \\
\dfrac{\partial U_1}{\partial \nu}\Big|_- = 0 & \text{on } \partial\Omega_1, \partial\Omega_2, \\
|U_1(x)| = O(|x|^{-1}) & \text{as } |x| \to \infty.
\end{cases}
$$

Consider $\Gamma_R^{(1,2)}$ the Green's function associated with Robin boundary conditions, that is defined for $x \in \mathbb{R}^2 \setminus (\overline{\Omega_1 \cup \Omega_2})$ by

(4.1)
$$
\begin{cases}
-\Delta_y \Gamma_R^{(1,2)}(x,y) = \delta_x(y), & y \in \mathbb{R}^2 \setminus \overline{\Omega_1 \cup \Omega_2}, \\
\Gamma_R^{(1,2)}(x,y)|_+ - \xi_1 \dfrac{\partial \Gamma_R^{(1,2)}}{\partial \nu_x}(x,y)\Big|_+ = 0, & y \in \partial\Omega_1, \\
\Gamma_R^{(1,2)}(x,y)|_+ - \xi_2 \dfrac{\partial \Gamma_R^{(1,2)}}{\partial \nu_x}(x,y)\Big|_+ = 0, & y \in \partial\Omega_2, \\
\left| \Gamma_R^{(1,2)}(x,y) + \dfrac{1}{2\pi}\log|y| \right| = O(|y|^{-1}), & |y| \to \infty.
\end{cases}
$$

Recall the following boundary integral equation: for each $x \in \mathbb{R}^2 \setminus (\overline{\Omega_1 \cup \Omega_2 \cup D})$,

$$
(u_1 - U_1)(x) = \int_{\partial D} \left(\frac{\partial u}{\partial \nu}\Big|_+ (y)\, \Gamma_R^{(1,2)}(x,y) - \frac{\partial \Gamma_R^{(1,2)}}{\partial \nu_y}(x,y)\, u|_+(y) \right) \mathrm{d}s_y,
$$

where U_1 is the background solution, i.e., the solution without the inhomogeneity D, when the only dipolar source lies inside the body of $\mathfrak{F}_1$, see Figure 2.4b.

$$
(u_1 - U_1)(x) = \frac{(k-1)}{k} \int_{\partial D} \left(\frac{\partial u}{\partial \nu}\Big|_+ (y)\, \Gamma_R^{(1,2)}(x,y) \right) \mathrm{d}s_y.
$$

Let B be a bounded open set with characteristic size 1. Assume that $D = z + \delta B$, i.e., D is a target located at z which has characteristic size δ. With the same argument as in [2], we obtain the following small volume approximation.

Theorem 4.1 (Dipolar approximation)*. Suppose $dist(\partial\Omega_1, z) \gg 1$ and $\delta \ll 1$. Then for any $x \in \partial\Omega_1$,*

$$(4.2) \qquad \left(\frac{\partial u_1}{\partial \nu} - \frac{\partial U_1}{\partial \nu}\right)(x) = -\delta^2 \nabla U_1(z)^T M(\lambda, B) \nabla_y \left(\left.\frac{\partial \Gamma_R^{(1,2)}}{\partial \nu}\right|_+\right)(x, z) + O(\delta^3),$$

where T denotes the transpose, $M(\lambda, B) = (m_{ij})_{i,j \in \{1,2\}}$ is the first-order polarization tensor associated with B and contrast parameter λ, given by

$$(4.3) \qquad m_{ij} = \int_{\partial B} y_i \left(\lambda I - \mathcal{K}_B^*\right)^{-1} \left(\left.\frac{\partial x_j}{\partial \nu}\right|_{\partial B}\right)(y) \; ds_y.$$

Note that, since the background potential is real, for $x \in \partial\Omega_1$ we have

$$(4.4) \qquad \mathrm{Im}\left(\frac{\partial u_1}{\partial \nu}\right)(x) \approx -\delta^2 \nabla U_1(z)^T \, \mathrm{Im}\, M(\lambda, B) \nabla_y \left(\left.\frac{\partial \Gamma_R^{(1,2)}}{\partial \nu}\right|_+\right)(x, z).$$

This last step is crucial to locate the target because U_1 is only approximately known from the measurements and even a very small displacement in the location of $\mathfrak{F}_2$ can cause an error on the background potential U_1, which is of the same order as the contribution of the target.

On the other hand, when z is not too close to $\partial\Omega_2$, the contribution of $\mathfrak{F}_2$ contained into $\nabla U_1(z)$ is negligible. Therefore, we approximate $\nabla U_1(z) \approx \nabla \widehat{U}_1(z)$, where $\widehat{U}_1$ is solution to the problem

$$(4.5) \qquad \begin{cases} \Delta\widehat{U}_1(x) = f_1(x) & \text{in } \Omega_1, \\ \Delta\widehat{U}_1(x) = 0 & \text{in } \mathbb{R}^2 \setminus \overline{\Omega_1}, \\ \widehat{U}_1|_+ - \widehat{U}_1|_- = \xi_1 \left.\dfrac{\partial\widehat{U}_1}{\partial\nu}\right|_+ & \text{on } \partial\Omega_1, \\ \left.\dfrac{\partial\widehat{U}_1}{\partial\nu}\right|_- = 0 & \text{on } \partial\Omega_1, \\ |\widehat{U}_1(x)| = O(|x|^{-1}) & \text{as } |x| \to \infty. \end{cases}$$

After post-processing (4.4) using the following operator

$$\mathcal{P}_{\Omega_1} = \frac{1}{2}I - \mathcal{K}_{\Omega_1}^* - \xi \frac{\partial \mathcal{D}_{\Omega_1}}{\partial \nu},$$

see [2], we get

$$(4.6) \qquad \mathcal{P}_{\Omega_1}\left[\mathrm{Im}\left(\frac{\partial u_1}{\partial \nu}\right)\right](x) \approx \delta^2 \nabla \widehat{U}_1(z)^T \, \mathrm{Im}\, M(\lambda, B) \nabla_y \left(\left.\frac{\partial \Gamma}{\partial \nu_x}\right|_+\right)(x, z), \quad x \in \partial\Omega_1.$$

Therefore, as long as $dist(z, \partial\Omega_2) \gg 0$, the leading order term of the post-processed measured data is not significantly affected by the presence of $\mathfrak{F}_2$.

A MUSIC-type algorithm for searching the position z and a least square method for recovering the imaginary part of the polarization tensor $M(\lambda, B)$ can be applied, see [4].

5. Numerical experiments

With applications in robotics in mind, and for the sake of simplicity, we can assume that the two fish populating our testing environment share the same effective thickness ξ and the same shape, which is an ellipse with semiaxes $a = 2$ and $b = 0.3$. Therefore no tail-bending has been taken into account.

For the numerical computations of the direct solutions to the transmission problems involved in the following simulations, we solved the boundary integral system of equations by relying on boundary element techniques. We adapted the codes in [38] to our framework, with many fish populating the same environment.

5.1. **Electro-communication.** We perform numerical simulations to show how $\mathfrak{F}_1$ can locate the position and the orientation of $\mathfrak{F}_2$ by using a modified version of MUSIC-type algorithm for searching the dipolar source. Firstly, let us observe that accuracy is not improved by using a multi-frequency approach when noisy measurements are considered. Instead, $\mathfrak{F}_1$ can use a MUSIC-type algorithm based on movement in order to improve the accuracy in the detection algorithm. We use the approximation (3.3).

We consider N_s positions. For each $s \in \{1, ..., N_s\}$ let us denote by $\mathfrak{F}_2^s$ the fish at the position s. On its skin there are N_r receptors $\{x_n^s\}_{n=1}^{N_r}$. For each $s = 1, ..., N_s$, we define the $M \times 2$ lead field matrix A_s as

$$(5.1) \qquad \mathbf{A}_s(z) = \begin{bmatrix} \dfrac{x_{1,1}^s - z_1}{\|x_1^s - z\|^2} & \dfrac{x_{1,2}^s - z_1}{\|x_1^s - z\|^2} \\ \vdots & \vdots \\ \dfrac{x_{M,1}^s - z_1}{\|x_M^s - z\|^2} & \dfrac{x_{M,2}^s - z_2}{\|x_M^s - z\|^2} \end{bmatrix}.$$

Let $\mathbf{F}$ be the Multi-Static Response (MSR) matrix defined as follows

$$\mathbf{F} = \begin{bmatrix} (u_2 - H^{u_2})(x_1^1) & \cdots & (u_2 - H^{u_2})(x_1^{N_s}) \\ \vdots & \ddots & \vdots \\ (u_2 - H^{u_2})(x_{N_r}^1) & \cdots & (u_2 - H^{u_2})(x_{N_r}^{N_s}) \end{bmatrix}.$$

Moreover, we assume that the acquired measurements are corrupted by noise, i.e.,

$$\mathbf{F}_{noisy} = \mathbf{F} + \mathbf{X},$$

where $\mathbf{X} \sim \mathcal{N}(0, \sigma_{\text{noise}}^2)$ is a Gaussian random variable with mean 0 and variance σ_{noise}^2. In our simulations we set the variance to:

$$\sigma_{\text{noise}} = (\mathbf{F}_{max} - \mathbf{F}_{min})\sigma_0,$$

where σ_0 is a positive constant called noise level, and $\mathbf{F}_{max}$ and $\mathbf{F}_{min}$ are the maximal and the minimal coefficient in the MSR matrix $\mathbf{F}$.

Let $\mathbf{F}_{noisy}^{\mathfrak{R}}$ be the real part of $\mathbf{F}_{noisy}$. Let $\lambda_1 \geq \lambda_2 \geq ... \geq \lambda_{N_r}$ be the eigenvalues of $\mathbf{F}_{noisy}^{\mathfrak{R}} \cdot (\mathbf{F}_{noisy}^{\mathfrak{R}})^T$ and let $\Phi_1, ..., \Phi_{N_r}$ be the correspondent eigenvectors. The first eigenvalue is the one associated to the signal source and the span of the eigenvector Φ_1 is called the signal subspace. The other eigenvectors span the noise subspace.

As it is well known, the MUSIC algorithm estimates the location of the dipole by checking the orthogonality between $\mathbf{A}_s(z)$ (5.1) and the noise subspace projector $\mathcal{P}_N$ [30]. This can be done for each position s.

For this purpose, we shall use a modified version of the MUSIC localizer in [34], by simply taking the maximum over the positions:

$$(5.2) \qquad \mathcal{I}_2(z) = \max_{s=1,...,N_s} \left(\frac{1}{\lambda_{\min}(\mathbf{A}_s(z)^T \mathcal{P}_N \mathbf{A}_s(z), \mathbf{A}_s(z)\mathbf{A}_s(z)^T)} \right),$$

where $\lambda_{\min}(\cdot, \cdot)$ indicates the generalized minimum eigenvalue of a matrix pair.

We expect that the MUSIC localizer has a large peak at the location of the equivalent dipole we are searching for. Once an estimate $\widehat{z}$ of the true location has been obtained, the dipole moment can be estimated by means of the following formula:
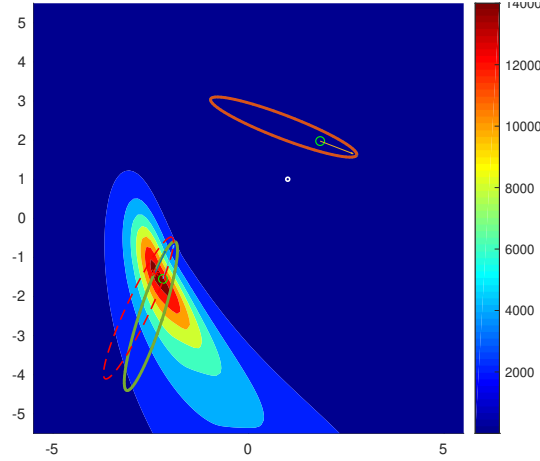
$$(5.3) \qquad \widehat{\mathbf{p}}_{est} = (\mathbf{A}(\widehat{z})^T\mathbf{A}(\widehat{z}))^{-1}\mathbf{A}(\widehat{z})^T\Phi_1.$$

i.e., the least-square solution to the linear system

$$(5.4) \qquad \Phi_1 = \mathbf{A}(\widehat{z})\widehat{\mathbf{p}}.$$
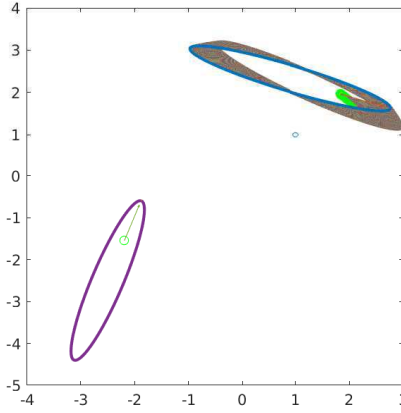
Figure 5.1. The setting. $\mathfrak{F}_1$ is acquiring measurements at $N_s = 150$ different closely spaced positions.

Figure 5.2. Estimate of the position and the orientation of $\mathfrak{F}_2$, with noise level $\sigma_0 = 0.1$. The dashed red curve represents the estimated body of $\mathfrak{F}_2$, whereas the green one represents the true body of $\mathfrak{F}_2$. The white circle represents a small dielectric object placed between $\mathfrak{F}_1$ and $\mathfrak{F}_2$.

Algorithm 1: MS MUSIC: Detect the presence of a conspecific from skin measurements

---

    Input : The feedback, that is the total electric potential signal $u(x,t)$ recorded by the receptors on $\partial\Omega_1$.

1 Decompose the feedback u into u_1 and u_2 using signal separation techniques;

2 MUSIC_dipoleSearch$(u_2|_{\partial\Omega_1}, \Omega_1)$:

3   Build the (real part of the) MSR matrix $\mathbf{F}_{noisy} \in M(N_r \times N_s, \mathbb{R})$ from measurements collected during a short period;

4   Compute the eigen-decomposition of $\mathbf{F}_{noisy}\mathbf{F}_{noisy}^T = \Phi\Lambda\Phi^T$ and the noise subspace projector $\mathcal{P}_N$;

5   Evaluate the MUSIC localizer $\mathcal{I}_2$ on the nodes of a fine uniform grid $\mathcal{G}$ in the vicinity of Ω_1 ;

6 $\widehat{z} \leftarrow \arg\max_{\mathcal{G}} \mathcal{I}_2(z)$;

7   Determine $\widehat{\mathbf{p}}_{est}$ as the least-square solution to the linear system (5.4);

    Output: an approximated position of the position of the electric organ of the conspecific $\mathfrak{F}_2$.

5.2. **Tracking.** Now we want to show that the dipole approximation that we assumed in the previous subsection is good enough to be used successfully for tracking purposes.

We assume the following setting for the numerical simulations. The fish $\mathfrak{F}_1$ is swimming along a fixed trajectory. Let us assume that the motion of its electric organ is described by a continuous path $F : [t_1, t_N] \longrightarrow \mathbb{R}^2$. Let $t_1 < t_2 < ... < t_N$ be a temporal grid on $[t_1, t_N]$ and let $t_j = s_1^j < ... < s_M^j = t_{j+1}$ be a grid on $[t_j, t_{j+1}]$ for $j = 1, ..., N-1$.

At the beginning, when $t = t_1$, $\mathfrak{F}_2$ starts following $\mathfrak{F}_1$. The tracking is performed by estimating the positions of $\mathfrak{F}_1$ at the nodes of the grid $t_1, ..., t_N$. Let us denote by X_n, Y_n and p_n, q_n the positions and the orientations of $\mathfrak{F}_2$ and $\mathfrak{F}_1$ at $t = t_n$, respectively. In order to obtain an estimate $\widehat{Y}_n$ of the position Y_n we can apply Algorithm 2, that employs measurements at $s_1^{n-1}, ..., s_M^{n-1}$ to reduce the effect of the noise. More precisely, the discrete dynamic system that describes the evolution of the positions and orientations of the two fish is as follows:

$$(5.5) \quad \begin{cases} X_n = X_{n-1} + h_n p_{n-1}, \\ p_n = \mathbf{R}(\theta_n)p_{n-1}, \\ Y_n = F(t_n), \\ q_n = F'(t_n) \approx \frac{F(t_n) - F(t_{n-1})}{h}, \end{cases}$$

where X_0 and p_0 are the initial data. Let us define $T_{n-1} := \widehat{Y}_{n-1} - X_{n-1}$, the pointing direction. The update of the orientation of $\mathfrak{F}_2$ is given by an orthogonal matrix associated with a rotation by an angle θ_n, $\mathbf{R}(\theta_n) \in O(2, \mathbb{R})$, and the turning angle is defined as

$$(5.6) \quad \theta_n := \theta_{n-1} \pm \min\left(\theta_{\max}, \widehat{T_{n-1}p_{n-1}}\right).$$

The numbers $h_1, ..., h_M$ incorporate the velocity of the tracking fish and should be chosen adaptively, in order to allow a variety of maneuvering capabilities such as acceleration and deceleration, as well as swimming backwards when $h_n < 0$. In order to prevent both collision and separation, we shall assume the velocity to be a function of the distance

between X_n and $\widehat{Y}_n$. $\theta_{\max}$ is the maximum turning angle. It is worth mentioning that the choice of $\theta_{\max}$ has a strong impact on the efficiency of the tracking procedure.

Algorithm 2: Real-Time Tracking: Fish-follows-Fish algorithm.

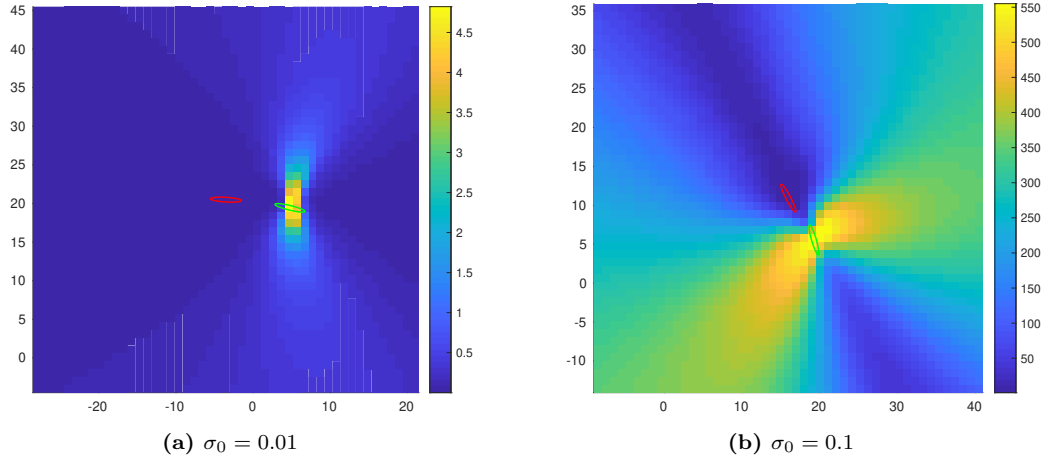   **Input** : Temporal grid over $[t_1, t_N]$. The maximum turning angle $\theta_{\max}$.

1 RT_Tracking($\theta_{\max}, [t_1, t_N], N, M$) :
2   **for** $n \leftarrow 1, \ldots, N$ **do**
3 $X_n \leftarrow X_{n-1} + h_n p_{n-1}$;
4 $p_n \leftarrow \mathbf{R}(\theta_n) p_{n-1}$;
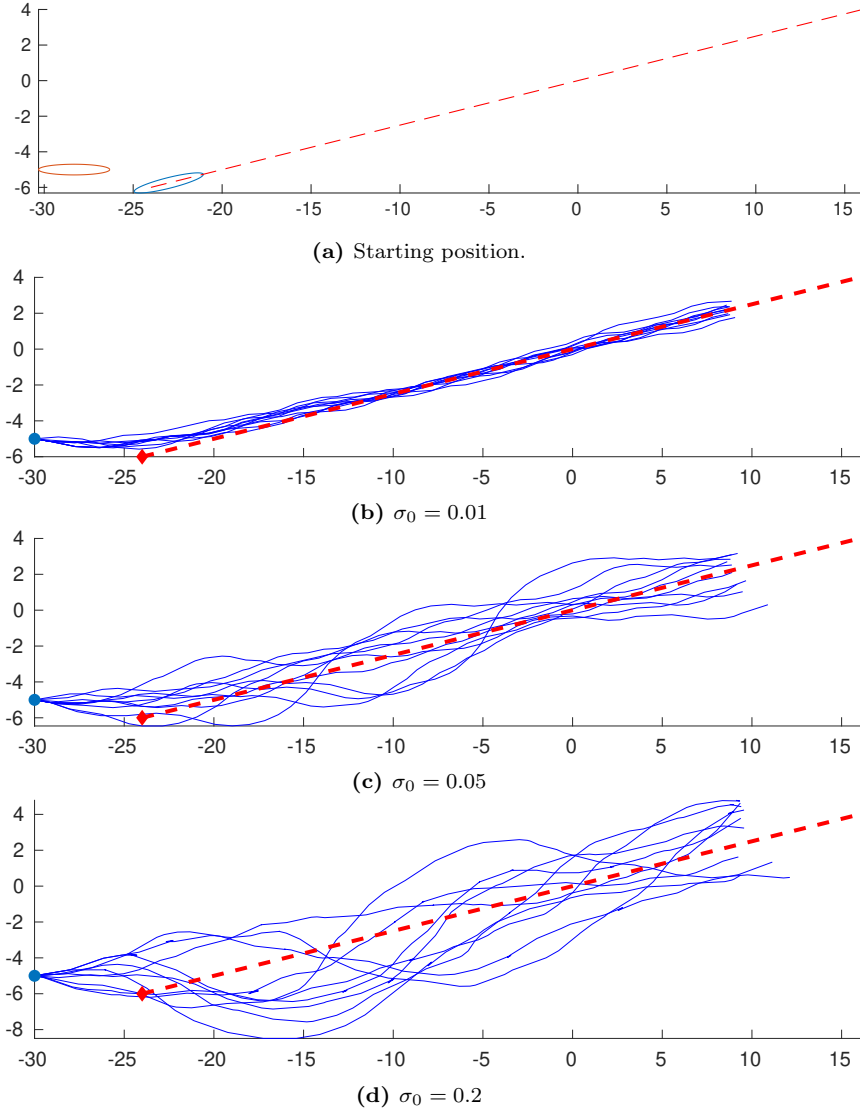**5** $\widehat{Y}_n \leftarrow$ MUSIC_dipoleSearch(n)
    end

          Output: Trajectory of the following fish.

(a) $\sigma_0 = 0.01$ **(b)** $\sigma_0 = 0.1$

Figure 5.3. Plot of the imaging functional $\mathcal{I}_2$ that the fish $\mathfrak{F}_1$ uses to track $\mathfrak{F}_2$.

(a) Starting position.

(b) $\sigma_0 = 0.01$

(c) $\sigma_0 = 0.05$

(d) $\sigma_0 = 0.2$
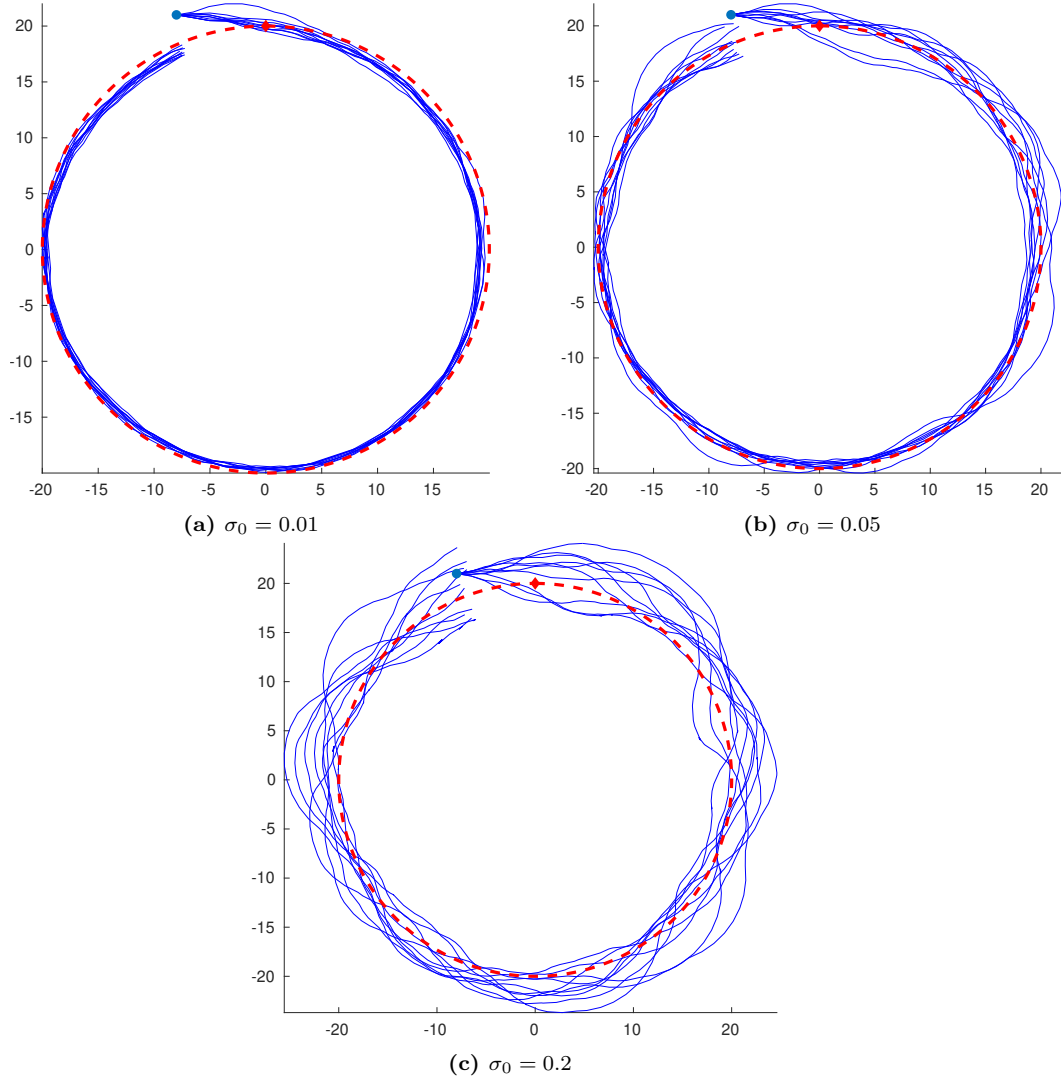
Figure 5.4. Plot of the linear trajectory tracking. $N_{\exp} = 10$ trials have been considered.

The algorithm `MUSIC_dipoleSearch` employs a multi-position dipole search that uses M positions in between. In our numerical simulations, in order to have a real-time tracking procedure, we have set $M = 5$. We have set $\theta_{\max} = 10^{-1}$.

5.3. **Electro-sensing.** While the fish can sense the presence of other conspecifics at some distance, the range for the active electrosensing is much more short [25].

The effectivity of the estimated position of a small dielectric target inevitably depends on the relative distances among the fish, its conspecifics and the target. However, this seems perfectly reasonable. We have to require

(a) $\sigma_0 = 0.01$

(b) $\sigma_0 = 0.05$

(c) $\sigma_0 = 0.2$

Figure 5.5. Plot of the trajectory tracking when the leading fish is swimming in circle, clockwisely. $N_{\exp} = 10$ trials/realizations have been considered.

(1) The two fish do not get too close to each other;
(2) The small dielectric target D is in the electro-sensing range of $\mathfrak{F}_1$.

If the above qualitative conditions are not met, there is no garantee that we can get accurate results.

We perform many experiments to show that the MUSIC-type algorithm proposed in [2] works under the conditions outlined above. Based on approximation (4.6) we consider the illumination vector

$$g(z) = \left(\nabla \widehat{U}_1(z) \cdot \nabla_z \left(\frac{\partial \Gamma}{\partial \nu_x} \right)(x_1, z), \ldots, \nabla \widehat{U}_1(z) \cdot \nabla_z \left(\frac{\partial \Gamma}{\partial \nu_x} \right)(x_{N_r}, z) \right)^T,$$

and define the MUSIC localizer as follows:

(5.7) $$\mathcal{I}_1(z) = \frac{1}{|(I - P)\widetilde{g}(z)|},$$

where $\widetilde{g} = \frac{g}{|g|}$ and $\widehat{U}_1$ is the solution to (4.5).

**Algorithm 3:** SF MUSIC: Detection of a small dielectric target in the presence of another conspecific

---

    Input **:** The feedback, that is the total electric potential signal $u(x,t)$ recorded by the receptors on $\partial\Omega_1$.

1 Decompose the feedback u into u_1 and u_2 using signal separation techniques ;

2 MUSIC_target$(u_1|_{\partial\Omega_1}, \Omega_1)$:

3   Post-process the data $\operatorname{Im} u_1|_{\partial\Omega_1}$;

4   Build the SFR $\mathbf{S}_{noise}$ for the post-processed data ;

5   Build and evaluate the MUSIC localizer $\mathcal{I}_1$ on the nodes of a fine uniform grid $\mathcal{G}$ in the vicinity of Ω_1 ;

6 $\widehat{z} \leftarrow \arg\max_{\mathcal{G}} \mathcal{I}_1(z)$;

    Output: An approximated position of the target.

(a) Plot of $\operatorname{Re} u_1$.   (b) Plot of $\operatorname{Im} u_1$.
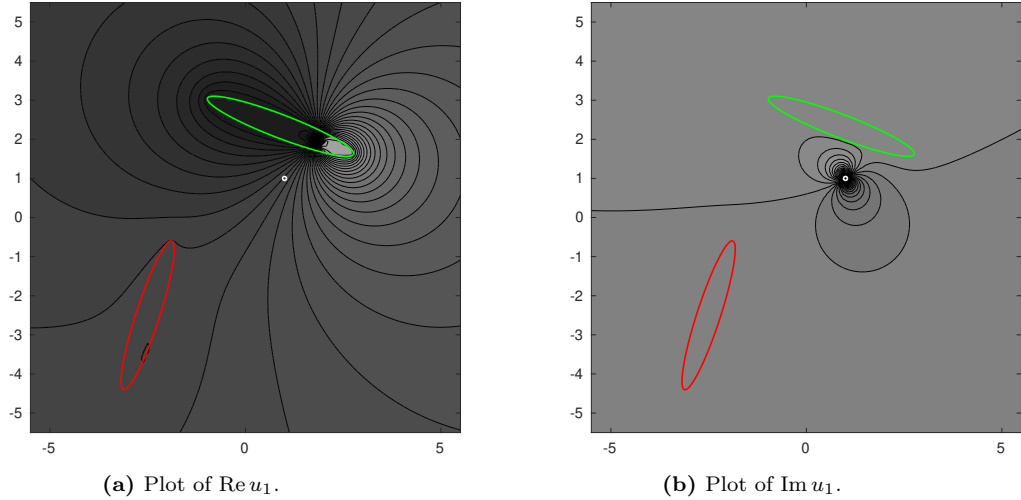
Figure 5.6. Plot of the isopotential lines when $\mathfrak{F}_2$ (red) is passive (electrically silent) and $\mathfrak{F}_1$ (green) is active.
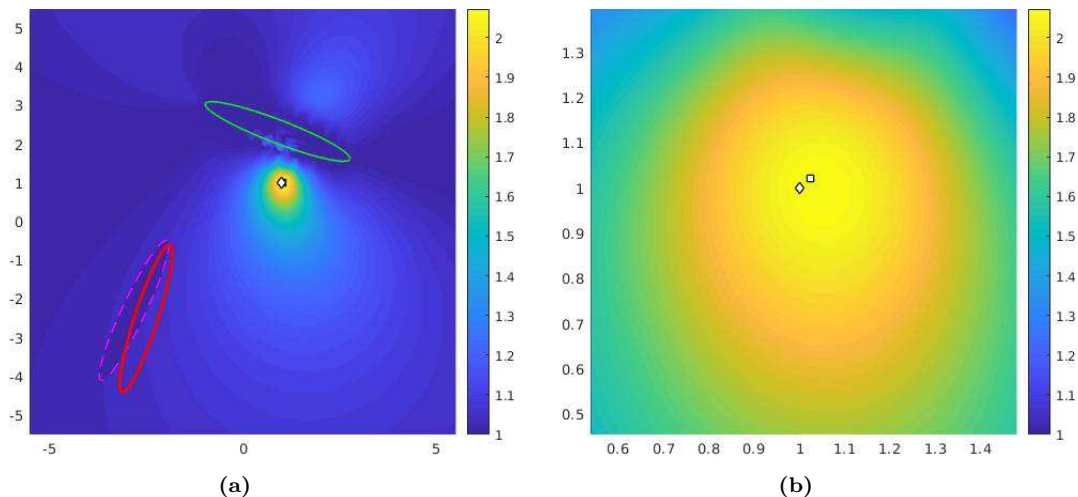
Figure 5.7. Plot of the MUSIC imaging functional used in Algorithm 3 by using $N_r = 32$ receptors and $N_f = 100$ frequencies, with noise level $\sigma_0 = 0.1$. The square and the diamond indicate the approximation of the center and the true center of the target D, respectively. $\mathfrak{F}_1$ (green) can image the target despite the presence of $\mathfrak{F}_2$ (red), which is estimated by applying Algorithm 2.

6. Concluding remarks

In this paper, we have formulated the time-domain model for a shoal of weakly electric fish. We have shown how the jamming avoidance response can be interpreted within this mathematical framework and how it can be exploited to design communication systems, following strategies and active electrosensing algorithms. In a forthcoming paper, we plan to extend our present approach to develop navigation patterns inspired by the collective behavior of the weakly electric fish.

7. Acknowledgment

References

[1] H. Ammari, *An Introduction to Mathematics of Emerging Biomedical Imaging*, Math. & Appl. 62. Springer, Berlin, 2008.

[2] H. Ammari, T. Boulier, and J. Garnier, Modeling active electrolocation in weakly electric fish, SIAM J. Imaging Sci., 6 (2013), 285–321.

[3] H. Ammari, T. Boulier, J. Garnier, W. Jing, H. Kang, and H. Wang, Target identification using dictionary matching of generalized polarization tensors, Found. Comput. Math., 14 (2014), 27–62.

[4] H. Ammari, T. Boulier, J. Garnier, and H. Wang, Shape recognition and classification in electrosensing, Proc. Natl. Acad. Sci. USA, 111 (2014), 11652–11657.

[5] H. Ammari, T. Boulier, J. Garnier, and H. Wang, Mathematical modelling of the electric sense of fish: the Role of multi-frequency measurements and movement, Bioinspir. Biomim., 12 (2017), 025002.

[6] H. Ammari, J. Garnier, H. Kang, M. Lim, and S. Yu, Generalized polarization tensors for shape description, Numer. Math. 126 (2014), no. 2,199–224.

[7] H. Ammari, M. Putinar, A. Steenkamp et al, Identification of an algebraic domain in two dimensions from a finite number of its generalized polarization tensors, Math. Ann. (2018).

[8] C. Assad, Electric field maps and boundary element simulations of electrolocation in weakly electric fish, PhD thesis, 1997 (California Institute of Technology, Pasadena, CA).

[9] D. Babineau, A. Longtin, and J.E. Lewis, Modeling the electric field of weakly electric fish, J. Exp. Biol., 209 (2006), 3636–3651.

[10] Y. Bai, I.D. Neveln, M. Peshkin, and M.A. MacIver, Enhanced detection performance in electrosense through capacitive sensing, Bioinspir. Biomim., 11 (2016), 055001.

[11] E. Bonnetier, F. Triki, and C.-H. Tsou, On the electro-sensing of weakly electric fish, J. Math. Anal. Appl., 464 (2018), 280–303.

[12] R. Budelli and A.A. Caputi, The electric image in weakly electric fish: Perception of objects of complex impedance, J. Exp. Biol., 203 (2000), 481–492.

[13] T .H. Bullock, R.H. Hamstra, H. Scheich, The jamming avoidance response of high frequency electric fish. J. Comp. Physiol. 77, 1-48 (1972).

[14] Angel Ariel Caputi, The bioinspiring potential of weakly electric fish, Bioinspir. Biomim., 12 (2017), 025004.

[15] A. A. Caputi, *Passive and active electroreception during agonistic encounters in the weakly electric fish Gymnotus omarorum*, Bioinspir. Biomim. 2016 Oct 21;11(6):065002.

[16] L. Chen, J.L. House, R. Krahe, and M.E. Nelson, Modeling signal and background components of electrosensory scenes, J. Comp. Physiol. A Neuroethol Sens Neural Behav. Physiol., 191 (2005), 331–345.

[17] M. Christensen, A. Jakobsson 2010. Optimal Filter Designs for Separating and Enhancing Periodic Signals. IEEE Transactions on Signal Processing. 58(12):5969-5983.

[18] O.M. Curet, N.A. Patankar, G.V. Lauder, and M.A. Maciver, Aquatic manoeuvering with counter-propagating waves: A novel locomotive strategy, J. R. Soc. Interface 8 (2011), 1041–1050.

[19] E Donati et al, Investigation of collective behaviour and electrocommunication in the weakly electric fish, Mormyrus rume, through a biomimetic robotic dummy fish, Bioinspiration & biomimetics 11 (6), 066009.

[20] B. He, T. Musha, Y. Okamoto, S. Homma, Y. Nakajima and T. Sato, *Electric Dipole Tracing in the Brain by Means of the Boundary Element Method and Its Accuracy*, in IEEE Transactions on Biomedical Engineering, vol. BME-34, no. 6, pp. 406-414, June 1987.

[21] W. Helligenberg, Theoretical and experimental approaches to spatial aspects of electrolocation, J. Comp. Physiol. A, 103 (1975), 247–272.

[22] W. Heiligenberg, Principles of Electrolocation and Jamming Avoidance in Electric Fish: A Neuroethological Approach. Studies of Brain Function, Vol. 1. Berlin-New York: Springer-Verlag (1977).

[23] The jamming avoidance response in gymnotoid pulse-species: A mechanism to minimize the probability of pulse-train coincidence, Journal of Comparative Physiology 124(3):211-224 · September 1978.

[24] N. Hoshimiya, K. Shogen, T. Matsuo, and S. Chichibu, The Apteronotus EOD field: Waveform and EOD field simulation, J. Comp. Physiol. A., 135 (1980), 283–290.

[25] B. Kramer, (1996) Electroreception and communication in fishes. Progress in Zoology, 42. Gustav Fischer, Stuttgart.

[26] H.W. Lissmann and K.E. Machin, The mechanism of object location in gymnarchus niloticus and similar fish, J. Exp. Biol., 35 (1958), 451–486.

[27] M.A. Maciver, The computational neuroethology of weakly electric fish: Body modeling, motion analysis, and sensory signal estimation, PhD thesis, 2001 (University of Illinois at Urbana-Champaign, Champaign, IL).

[28] M.A. MacIver, N.M. Sharabash, and M.E. Nelson, Prey-capture behavior in gymnotid electric fish: Motion analysis and effects of water conductivity, J. Exp. Biol., 204 (2001), 543–557.

[29] P. Moller, Electric Fish: History and Behavior, 1995 (Chapman and Hall, London).

[30] J. C. Mosher, P. S. Lewis and R. M. Leahy, "Multiple dipole modeling and localization from spatio-temporal MEG data" in IEEE Transactions on Biomedical Engineering, vol. 39, no. 6, pp. 541-557, June 1992.

[31] M.E. Nelson, Target Detection, Image Analysis, and Modeling, 2005 (Springer-Verlag, New York).

[32] B. Rasnow, C. Assad, M.E. Nelson, and J.M. Bower, Simulation and measurement of the electric fields generated by weakly electric fish, Advances in Neural Information Processing Systems 1, ed Touretzky DS (Morgan Kaufmann Publishers, San Mateo, CA), pp. 436–443, 1989.

[33] A. Scapin, Electrosensing of inhomogeneous targets, to appear on Journal of Mathematical Analysis and Applications (2018).

[34] K. Sekihara, D. Poeppel, A. Marantz, H. Koizumi, Y. Miyashita, Noise covariance incorporated MEG-MUSIC algorithm: a method for multiple-dipole estimation tolerant of the influence of background

brain activity, in IEEE Transactions on Biomedical Engineering, vol. 44, no. 9, pp. 839-847, Sept. 1997.

[35] G. von der Emde, S. Schwarz, L. Gomez, R. Budelli, and K. Grant, Electric fish measure distance in the dark, Science, 260 (1993), 1617–1623.

[36] G. von der Emde G, and S. Fetz, Distance, shape and more: Recognition of object features during active electrolocation in a weakly electric fish, J. Exp. Biol. 210 (2007), 3082–3095.

[37] G. von der Emde, Active electrolocation of objects in weakly electric fish, J. Exp. Biol., 202 (1999), 1205–1215.

[38] H. Wang, Shape identification in electro-sensing, https://github.com/yanncalec/SIES.

[39] W. Wang et al, A bio-inspired electrocommunication system for small underwater robots, 2017 Bioinspir. Biomim. 12.

[40] X. Zheng, Artificial lateral line based local sensing between two adjacent robotic fish, Bioinspir. Biomim. 2017 Nov 27;13(1):016002.

DEPARTMENT OF MATHEMATICS, ETH ZÜRICH, RÄMISTRASSE 101, CH-8092 ZÜRICH, SWITZERLAND.
Email address: andrea.scapin@sam.math.ethz.ch